Supplement of Atmos. Chem. Phys., 24, 6153–6175, 2024
https://doi.org/10.5194/acp-24-6153-2024-supplement

Atmospheric Chemistry and Physics
Open Access

Supplement of

Observation-constrained kinetic modeling of isoprene SOA formation in the atmosphere

Chuanyang Shen et al.

Correspondence to: Haofei Zhang (haofei.zhang@ucr.edu)

Text S1:

Reactive uptake

The reactive uptake coefficient (for epoxides, lactone, and alkylnitrates) can be described as the following equation:

$$\frac{1}{\gamma} = \frac{r_p \omega}{4D_{gas}} + \frac{1}{\alpha} + \frac{1}{\Gamma_{aq}}$$

The α is 0.02; D_{gas} is 0.1cm^2 s^{-1}; Γ_{aq} is calculated from the following equation:

$$\Gamma_{aq} = \frac{4\,VRTH_{aq}k_{aq}}{SA * \omega}$$

for IEPOX, the ω is 2.81×10^4 cm s^{-1}; for HMML, the ω is 2.69×10^8 cm s^{-1}; V is the total particle volume; R is the Universal gas constant of 0.08205 L atm mol^{-1} K^{-1}; for IEPOX, H_{aq} is 1.3×10^8 M atm^{-1}; for HMML, H_{aq} is estimated from EPI as 3.76×10^4 M atm^{-1}. The k_{aq} is calculated as:

$$k_{aq} = \sum_{i=1}^{N}\sum_{j=1}^{M} k_{i,j}[nuc_i][acid_j]$$

[nuc] is the concentration of nucleophiles (M) and it can be either the water or sulfate, [acid] is the concentration of acids (M). All these parameters can be modeled using the ISORROPIA II. a_{H^+} is the proton activity, and the $k_{i,j}$ is shown in the Table S8. In the model, we assume that the reactive uptake of all epoxides follows the same reaction kinetics, that means the k_{i,H^+} and $k_{i,HSO4^-}$ are the same for IEPOX, MGA and other epoxides. But the H_{aq} values are different given by the EPI estimation.

Text S2:

The model setup for different chamber experiments

UNC-2010/2012:

In UNC-2010/2012, a total of 23 experiments were performed at the University of North Carolina 270 m^3 dual outdoor smog chamber under clear natural sunlight. Overall, the initial NO_x/isoprene ratios varied from 0.06 to 0.53, with initial isoprene concentration ranging from 200 ppb to 1250 ppb. The concentrations of O_3, NO_x and isoprene were measured from the chamber and the experimental facility can be referred to in previous studies (Kamens et al., 2011; Zhang et al., 2011; Zhang et al., 2013). The experimental conditions for all these 23 experiments are summarized in Table S3. J values, temperature (T) and RH are derived from real-time measurements. The simulation is run in gas mode, which means only the gas-phase reactions are allowed.

Kroll-2006:

Kroll-2006 included 8 unseeded NO_x-free experiments and 6 seeded high-NO_x experiments. The initial isoprene concentration varied from 12.2 ppb to 90 ppb for NO_x-free experiments. The initial NO_x/isoprene ratios spanned a wide range from 1 to 16.9 with initial isoprene concentration around 45 ppb for high-NO_x experiments. The input values are shown in Table S4. The chamber RH in the meteorology field is 50%. The J_{NO2}, J_{NO3NO}, J_{NO3NO2}, and J_{H2O2} are 0.0048, 2×10^{-4}, 4.6×10^{-4} and 2.9×10^{-6} s^{-1}, respectively (Thornton et al., 2020). Other J values are calculated from solar zenith angle (SZA=50) using MCM's solar zenith angle parameterization. The C* threshold is set as 100 μg m^{-3}, which means that species with C* >100 μg m^{-3} are excluded from contributing to SOA formation and species otherwise will go through gas-particle partitioning to form the SOA. Since the SOA measurements in our simulated chamber studies have been corrected for losses of

particles to walls, the model simulation does not include particle wall loss. For the vapor wall loss, it was treated based on Zhang et al. (2014). The threshold to invoke wall partitioning is 1×10^{6} μg m^{-3}; The equivalent absorbing organic mass concentration of the wall material is set as 1×10^{4} μg m^{-3}; and the timescale to mix vapors to wall surface is set as 2.5×10^{-4} s^{-1}.

PNNL-2018:

The initial concentrations include isoprene, H_2O_2, NO, NO_2. The input values are shown in Table S4. The chamber RH in the meteorology field is 5%. The J_{NO2}, J_{NO3NO}, J_{NO3NO2}, and J_{H2O2} are 0.006, 2×10^{-4}, 4.6×10^{-4} and 2.2×10^{-6} s^{-1}, respectively. Other J values are calculated from solar zenith angle (SZA=50). The C* threshold is set as 100 μg m^{-3}. No particle wall loss is included in the model simulation. A first-order rate coefficient for irreversible vapor wall loss of 1×10^{-4} s^{-1} is applied in the model.

PNNL-2014:

The initial concentrations include isoprene, H_2O_2 and NO, which are shown in Table S4. The initial NO_x/isoprene ratios were 0-3.8. The J_{NO2} and J_{H2O2} are 0.006 s^{-1} and 2.5×10^{-6} s^{-1}, respectively. SZA is set to 50 and is used to calculate other J values. The experiments were conducted in the continuous-flow steady-state mode in which reacts were continuously injected into the chamber and the total flow into and out of the chamber is balanced, so the dilution factor is set to 5.6×10^{-5} s^{-1} and continuous injections of isoprene, H_2O_2 and NO into the chamber are included in the model. The C* threshold is set as 100 μgm^{-3}. Wall loss rate is set as 6×10^{-5} s^{-1}. A first-order rate coefficient for irreversible vapor wall loss of 1×10^{-4} s^{-1} is applied in the model (Thornton et al., 2020).

Schwantes-2019:

The initial concentrations include isoprene, CHO_3NO, NO, NO_2. The input values are shown in Table S5. The initial NO_x/isoprene ratios were 8.7-13.2. The J_{NO2} is set as 4×10^{-4} s^{-1} and the other J values are calculated from solar zenith angle (SZA=84.525), which can best fit the J_{NO2}. The C* threshold is set as 100 μg m^{-3}. The model simulation doesn't include particle wall loss. The threshold to invoke wall partitioning is 1×10^{6} μg m^{-3}; The equivalent absorbing organic mass concentration of the wall material is set as 1×10^{4} μg m^{-3}; and the timescale to mix vapors to wall surface is set as 2.5×10^{-4} s^{-1}.

Ng-2008:

Ng-2008 were performed in the dark at room temperature and under dry conditions (RH<10%) using N_2O_5 as a source of NO_3 radicals. The initial isoprene concentration was 18.4-101.6 ppb and seed aerosols are introduced into the chamber for most experiments. The initial concentrations include isoprene and N_2O_5, as shown in Table S6. For these nighttime oxidation simulations, the SZA is set as 90. For the vapor wall loss, the threshold to invoke wall partitioning is 1×10^{6} μg m^{-3}; The equivalent absorbing organic mass concentration of the wall material is set as 1×10^{4} μg m^{-3}; and the timescale to mix vapors to wall surface is set as 2.5×10^{-4} s^{-1}. No particle wall loss is included in the model simulation.

Schwantes-2015:

Only the Experiment 8 in the reference is simulated here. The initial concentrations include isoprene (24 ppb), NO_2 (100 ppb), HCHO (4 ppm) and O_3 (49 ppb). The SZA is set as 90 and all the J values are 0, corresponding to nighttime oxidation.

Carlsson-2023:

The initial concentrations include: O_3, NO_2, isoprene, NO_3. The input values are shown in Table S7. The temperature was set as 292 K. The SZA is set as 90, so all the J values are 0 corresponding to nighttime oxidation.

Table S1. Abbreviated names and descriptions of species appearing in the UCR-ISOP mechanism.

Abbreviated Name	Description
ISOP	Isoprene
MACR	Methacrolein
MVK	Methyl vinyl ketone
IEPOXOO	Peroxy radicals formed from IEPOX
NISOPO2	Lumped isoprene nitrooxy peroxy radicals
NIT1NO3OOA	Peroxy radicals formed from NIT1 oxidation (OH-abstraction of the aldehydic hydrogen atom)
NIT1OHOO	Peroxy radicals formed from isoprene 1-hydroxy nitrates
IMACO3	Peroxymethacryl radical (CH_2=C(CH_3)C(O)O_2)
MACROO	Lumped peroxy radicals produced from MACR oxidation (OH addition)
MVKOO	Lumped peroxy radicals produced from MVK oxidation (OH addition)
HC5	C5 hydroxy carbonyls
NIT1	Lumped isoprene carbonyl nitrates
NISOPOOH	Lumped isoprene hydroperoxyl nitrates
MACRN	Lumped MACR nitrate
MVKN	Lumped MVK nitrate
IMPAA	methacrylic peracid
IMAPAN	Methacryloyl peroxynitrate
IMAE	Methacrylic acid epoxide
IHMML	Hydroxymethyl-methyl-alpha-lactone
PYRUACD	Pyruvic acid
HPALD1	Lumped Z-hydroperoxy-methyl-butenals
HPALD2	Isoprene hydroperoxy aldehydes
ISOPOOH12	1,2-isoprene hydroxy hydroperoxides
ISOPOOH43	4,3-isoprene hydroxy hydroperoxides
ISOPOOHD	Delta isoprene hydroxy hydroperoxides
IEPOXB	1,4-dihydroxy epoxides
IEPOXD	3,4-dihydroxy epoxides
ISOP1OH2N	1,2-isoprene-derived hydroxy nitrate
ISOP3N4OH	4,3-isoprene-derived hydroxy nitrate
ISOPHND	Isoprene-derived hydroxy nitrates
IDH	Lumped isoprene dihydroxy products
IDC	Lumped isoprene dicarbonyls
IDN	Lumped isoprene dinitrates
ICHE	Lumped isoprene C5 oxidation products with 1 carbonyl, 1 hydroxy and 1 epoxide functional group
IDHPE	Lumped isoprene C5 oxidation products with 2 hydroxy, 1 hydroperoxide and 1 epoxide functional group
IDNE	Isoprene dinitrate epoxides
IHPE	Lumped isoprene hydroxy hydroperoxyl epoxides

IHNE	Lumped isoprene hydroxy nitrate epoxides
INPE	Lumped isoprene nitrate hydroperoxyl epoxides
ICNE	Lumped isoprene carbonyl nitrate epoxides
ICPE	Lumped isoprene carbonyl hydroperoxyl epoxides
IHNPE	Lumped isoprene hydroxy nitrate hydroperoxyl epoxides
ICPDH	Lumped isoprene C5 oxidation products with 1 carbonyl, 1 hydroperoxide and 2 hydroxy functional groups
IDHDP	Lumped isoprene dihydroxy dihydroperoxides
IDCHP	Lumped isoprene C5 oxidation products with 2 carbonyl, 1 hydroxy and 1 hydroperoxide functional group
ITHP	Lumped isoprene C5 oxidation products with 3 hydroxyl group and 1 hydroperoxide
ITHC	Lumped isoprene C5 oxidation products with 1 carbonyl and 3 hydroxyl functional groups
ICHNP	Lumped isoprene C5 oxidation products with 1 carbonyl, 1 hydroxy, and 1 epoxide functional group
IDHDN	Lumped isoprene C5 oxidation products with 2 hydroxy, 2 nitrate functional groups
IDHPN	Lumped isoprene C5 oxidation products with 2 hydroxy, 1 hydroperoxide and 1 nitrate functional group
IDHCN	Lumped isoprene C5 oxidation products with 2 hydroxy, 1 carbonyl and 1 nitrate functional group
ICHDN	Lumped isoprene C5 oxidation products with 1 carbonyl, 1 hydroxyl and 2 nitrate functional groups
ICDPN	Lumped isoprene C5 oxidation products with 1 carbonyl, 2 hydroperoxide and 1 nitrate functional group
IHPDN	Lumped isoprene C5 oxidation products with 1 hydroxy, 1 hydroperoxide and 2 nitrate functional groups
IHNDP	Lumped isoprene C5 oxidation products with 1 hydroxy, 1 nitrate and 2 hydroperoxide functional groups
IHNDC	Lumped isoprene C5 oxidation products with 1 hydroxy, 1 nitrate and 2 carbonyl functional groups
ITHN	Lumped isoprene C5 oxidation products with 3 hydroxy and 1 nitrate functional group
INPA	Lumped isoprene C5 oxidation products with 1 nitrate, 1 hydroperoxide and 1 carboxyl group
INCA	Lumped isoprene C5 oxidation products with 1 nitrate, 1 carbonyl and 1 carboxyl group
C4HP	Lumped hydroxy hydroperoxides produced from MACR and MVK oxidation
C4HC	Lumped hydroxy carbonyls produced from MACR and MVK oxidation
C4DH	Lumped dihydroxy oxidation products from MACR and MVK
C4ENOL	Lumped C4 enols from MACR and MVK

C4PN	Lumped hydroperoxyl nitrates produced from MACR and MVK oxidation
HPETHNL	(Hydroperoxy) ethanal
HPAC	Peroxylacetone
MGA	2-Methylglyceric acid produced from MACR oxidation (OH addition)
NMGA	2-Methylglyceric acid nitrate form produced from MACR oxidation (OH addition)
C10dimer	The dimer products formed from RO2 with RO2
ISOP1OHOO	Lumped isoprene 1-hydroxy peroxy radicals
ISOP4OHOO	Lumped isoprene 4-hydroxy peroxy radicals
ISOPOOHOO	Peroxy radicals formed from ISOPOOH oxidation (OH addition)
NIEPOXOO	Nitrated epoxy peroxy radicals
ISOPNOO	Peroxy radicals produced from INTR oxidation
IHDNOO	As above, but from IHDN
IHPNOO	As above, but from IHPN

110
111

Table S2. The C^* values under the temperature of 298K for the semi-volatile and low-volatile species in ISOP-UCR mechanism. One name in the ISOP-UCR mechanism may correspond to several isomers whose SMILES (simplified molecular-input line-entry system) and C^* values are listed in the table too. In the calculation of gas-particle partitioning, the lowest C^* value in the isomers is used.

Names	Formula	SMILES	C^*_Evaporation ($\mu g\ cm^{-3}$)	C^*_SIMPOL.1 ($\mu g\ cm^{-3}$)
IDHPE	$C_5H_{10}O_5$	CC(CO)(OO)C1OC1O	15.87	103.00
		CC1(C(CO)OO)[O]C1O	15.87	
IDHDP	$C_5H_{12}O_6$	CC(CO)(OO)C(CO)OO	0.03	2.03
		CC(CO)(OO)C(O)COO	0.14	
		CC(O)(COO)C(CO)OO	0.67	
ICPDH	$C_5H_{10}O_5$	OCC(C(C=O)(O)C)OO	244.11	24.00
		OOC(C=O)C(C)(O)CO	244.11	
		OCC(O)C(C)(OO)C=O	54.02	
		O=CC(O)C(C)(CO)OO	54.02	
		OCC(=O)C(C)(CO)OO	23.72	
IDHCN	$C_5H_9NO_6$	OCC(ON(=O)=O)C(C)(O)C=O	2599.78	51.43
		O=CC(C)(O)C(O)CON(=O)=O	9131.41	
		O=CC(O)C(C)(CO)ON(=O)=O	625.60	
		O=CC(O)C(C)(O)CON(=O)=O	9131.41	
		OCC(O)C(C)(C=O)ON(=O)=O	625.60	
		[O-][N+](=O)OC(C(CO)(O)C)C=O	2599.78	
IDCHP	$C_5H_8O_5$	CC(O)(C(=O)OO)C(=O)C	102097.15	8950.00
		OCC(C(=O)C)C(=O)OO	2454.80	
		OCC(OO)(C=O)C(=O)C	1045.76	418.00
		OCC(=O)C(C)(OO)C=O	3446.76	
ITHP	$C_5H_{12}O_5$	CC(O)(CO)C(CO)OO	2.34	3.33
		CC(CO)(OO)C(O)CO	0.49	
ITHC	$C_5H_{10}O_4$	CC(O)(CO)C(=O)CO	1461.84	93.60
		O=CC(CO)C(O)CO	24.46	38.70
IDHPN	$C_5H_{11}NO_7$	OCC(C)(OO)C(O)CON(=O)=O	1.77	4.29
		OCC(OO)C(C)(CO)ON(=O)=O	0.46	
		OOCC(O)C(C)(CO)ON(=O)=O	1.77	
		OCC(OO)C(C)(O)CON(=O)=O	8.00	
		OCC(ON(=O)=O)C(C)(CO)OO	0.46	
ICHNP	$C_5H_9NO_7$	OCC(ON(=O)=O)C(C)(OO)C=O	47.21	30.98
		OOC(C)(C=O)C(O)CON(=O)=O	165.74	
		OOC(C=O)C(C)(CO)ON(=O)=O	47.21	
		O=CC(O)C(C)(OO)CON(=O)=O	165.74	

		OCC(C(O[N+](=O)[O-])(C=O)C)OO	47.21	
		O=CC(C(OO)(CO)C)O[N+](=O)[O-]	47.21	
IDHDN	$C_5H_{10}N_2O_8$	OCC(ON(=O)=O)C(C)(CO)ON(=O)=O	5.62	8.83
		OCC(C)(ON(=O)=O)C(O)CON(=O)=O	19.74	
		OCC(ON(=O)=O)C(C)(O)CON(=O)=O	82.02	
ICHDN	$C_5H_8N_2O_8$	O=CC(ON(=O)=O)C(C)(CO)ON(=O)=O	492.21	64.04
		OCC(ON(=O)=O)C(C)(C=O)ON(=O)=O	492.21	
		O=CC(C)(ON(=O)=O)C(O)CON(=O)=O	1391.55	
		O=CC(ON(=O)=O)C(C)(O)CON(=O)=O	4786.72	
IHPDN	$C_5H_{10}N_2O_9$	CC(CO)(ON(=O)=O)C(COO)ON(=O)=O	1.46	5.24
		CC(COO)(ON(=O)=O)C(CO)ON(=O)=O	1.46	
		CC(COO)(ON(=O)=O)C(O)CON(=O)=O	5.14	
		CC(O)(CON(=O)=O)C(COO)ON(=O)=O	21.36	
IHNDP	$C_5H_{11}NO_8$	CC(CO)(OO)C(COO)ON(=O)=O	0.13	2.57
		CC(CO)(OO)C(CON(=O)=O)OO	0.13	
		CC(COO)(ON(=O)=O)C(CO)OO	0.13	
		CC(CON(=O)=O)(OO)C(CO)OO	0.13	
		CC(CO)(ON(=O)=O)C(COO)OO	0.13	
		CC(COO)(OO)C(CO)ON(=O)=O	0.13	
IHNDC	$C_5H_7NO_6$	O=CC(=O)C(C)(CO)ON(=O)=O	34628.29	896.43
		O=CC(O)C(C)(C=O)ON(=O)=O	50778.52	
		O=CC(=O)C(C)(O)CON(=O)=O	336740.22	
		O=CC(C(C=O)(O)C)O[N+](=O)[O-]	174659.59	
ITHN	$C_5H_{11}NO_6$	CC(O)(CO)C(CO)ON(=O)=O	29.08	7.11
		CC(CO)(ON(=O)=O)C(O)CO	6.44	
IHNPE	$C_5H_9NO_7$	O=N(=O)OCC1(COO)OC1CO	28.47	132.21
ICNE	$C_5H_7NO_5$	CC1(CON(=O)=O)OC1C=O	1282937.17	220289.06
INPE	$C_5H_9NO_6$	CC1(COO)OC1CON(=O)=O	12333.61	18569.88
IHNE	$C_5H_9NO_5$	CC1(CO)OC1CON(=O)=O	50430.41	30557.83
ICPE	$C_5H_8O_4$	CC1(COO)OC1C=O	364022.82	101000.00
ICHE	$C_5H_8O_3$	CC1(CO)OC1C=O	14117988.17	160000.00

IDNE	$C_5H_8N_2O_7$	CC1(CON(=O)=O)OC1CON(=O)=O	42133.98	38763.39
IHPE	$C_5H_{10}O_4$	CC1(COO)OC1CO	16317.00	13969.74
INPA	$C_5H_7NO_6$	CC(=CC(=O)OO)CON(=O)=O	40944.98	71687.98
INCA	$C_5H_7NO_5$	CC(=CC(=O)O)CON(=O)=O	4509.29	5389.39

118

Table S3. The initial conditions of UNC chamber experiments.

Run	[isoprene] (ppb)	[NO] (ppb)	[NO_2] (ppb)	[NO_x] (ppb)	[isoprene]/[NO_x]
20090701N	400	159.9	29.6	189.5	2.11
20090703N	400	183.1	26	209.1	1.91
20090703S	400	95.6	22.6	118.2	3.38
20100622N	1100	91.2	26.3	117.5	9.36
20100622S	1250	185.8	50.1	235.9	5.30
20100705N	410	93.8	5.3	99.1	4.14
20100904N	950	29.1	24.6	53.7	17.69
20100904S	800	104.4	30.3	134.7	5.94
20101015N	400	142	9	151	2.65
20101015S	430	138.3	0.1	138.4	3.11
20101021N	790	253.4	0.1	253.5	3.12
20101021S	800	252	0	252	3.17
20110630S	392	94.4	32.2	126.6	3.10
20120531S	950	209.5	36.3	245.8	3.86
20120603N	780	65.2	38.7	103.9	7.51
20120603S	590	66.6	38.7	105.3	5.60
20120608N	1000	73.7	29	102.7	9.74
20120608S	370	74.7	29.5	104.2	3.55
20120628S	200	68.8	31.5	100.3	1.99
20120630N	760	141.7	49	190.7	3.99
20120630S	680	141.4	49.6	191	3.56
20120705N	980	163	23.8	186.8	5.25
20120705S	410	162.6	25.9	188.5	2.18

Table S4. The initial conditions of Kroll-2006 and PNNL-2018 experiments.

Chamber	Run	[isoprene] (ppb)	[H_2O_2] (ppm)	[NO] (ppb)	[Seed] ($\mu m^3 cm^{-3}$)	T (°C)
Kroll-2006	1	90	3.5	0	N/A	25.4
	2	46.1	3.5	0	N/A	25.6
	3	23	3.5	0	N/A	26
	4	12.2	3.5	0	N/A	25.7
	5	63.6	3.5	0	N/A	26.7
	6	29.4	3.5	0	N/A	28.7
	7	47.8	3.5	0	N/A	26.6
	8	41.6	3.5	0	N/A	26.4
	9	46.7	3.5	242	4.6	28.3
	10	43.5	3.5	496	7.1	28.3
	11	42.7	3.5	98	6.4	28.1
	12	49.1	3.5	51	6.5	28.2
	13	42.7	3.5	337	4.8	28.3
	14	42	3.5	708	4.7	27.5
PNNL-2018	1	43.5	7.5	0	0.3	24
	2	65	7.5	0	0.3	24
	3	69	7.5	0	0.3	24
	4	56.5	7.5	0	0.3	24
	5	51	7.5	0	0.3	24
	6	57	7.5	0	0.3	24
	7	48	7.5	0	0.3	24
PNNL-2014	1	26	15	0	0.3	25.4
	2	26	10	0	0.3	25.4
	3	26	10	2	0.3	25.4
	4	26	10	5	0.3	25.4
	5	26	10	10	0.3	25.4
	6	26	10	20	0.3	25.4
	7	26	10	50	0.3	25.4

Table S5. The experimental conditions of Schwantes-2019 experiments.

Run	[isoprene] (ppb)	[NO] (ppb)	[NO_2] (ppb)	[CH_3ONO] (ppb)	[Seed] ($\mu m^3 cm^{-3}$)	T (°C)	RH (%)
1	59	585	6	118	0	25.6	5
2	58	526	20	117	54	26.4	5.6
3	57	519	17	117	183	25.9	7.5
4	58	518	18	116	337	26.4	7.9
5	55	506	20	117	159	12.8	16.4
6	56	541	16	118	152	32.4	5.9
7	40	527	18	117	197	25.9	8.1
8	60	519	20	118	109	25.5	44.7
9	55	489	20	119	166	25.6	78.1
10	58	516	17	111	85	25.8	5.1
11	56	490	17	115	264	25.8	5.2

Table S6. The experimental conditions of Ng-2008 experiments.

Run	[isoprene] (ppb)	[N_2O_5] (ppb)	T (°C)	RH (%)	SOA Yield (%)
1	101.6	1000	21	5.1	23.8
2	30.2	1000	20	4.7	13.5
3	67.1	1000	21	5.4	20.8
4	51.7	1000	20	6	18.2
5	18.4	1000	21	5.7	4.3
6	21.8	1000	21	5.5	7.8
7	39.5	1000	20	5.5	7.1
8	42	1000	21	6.4	14.1

Table S7. The experimental conditions of Carlsson-2023.

Run	[isoprene] (ppb)	[NO_3] (ppt)	[NO_2] (ppb)	[O_3] (ppb)	T (K)
1	2.4	5	5	101	297
2	1.69	40	4.5	100	295
3	2.5	3.5	12	78	295
4	4.4	250	25	105	292

Table S8. The parameters in the calculation of reactive uptake of IEPOX.

Product species	Parent species	Nucleophile	$k_{i,H^+}[M^{-2}s^{-1}]$	$k_{i,HSO4^-}[M^{-2}s^{-1}]$
2-MT	IEPOX	Water	2×10^{-4}	1.3×10^{-5}
IEPOX- OS	IEPOX	Sulfate	2×10^{-4}	2.9×10^{-6}

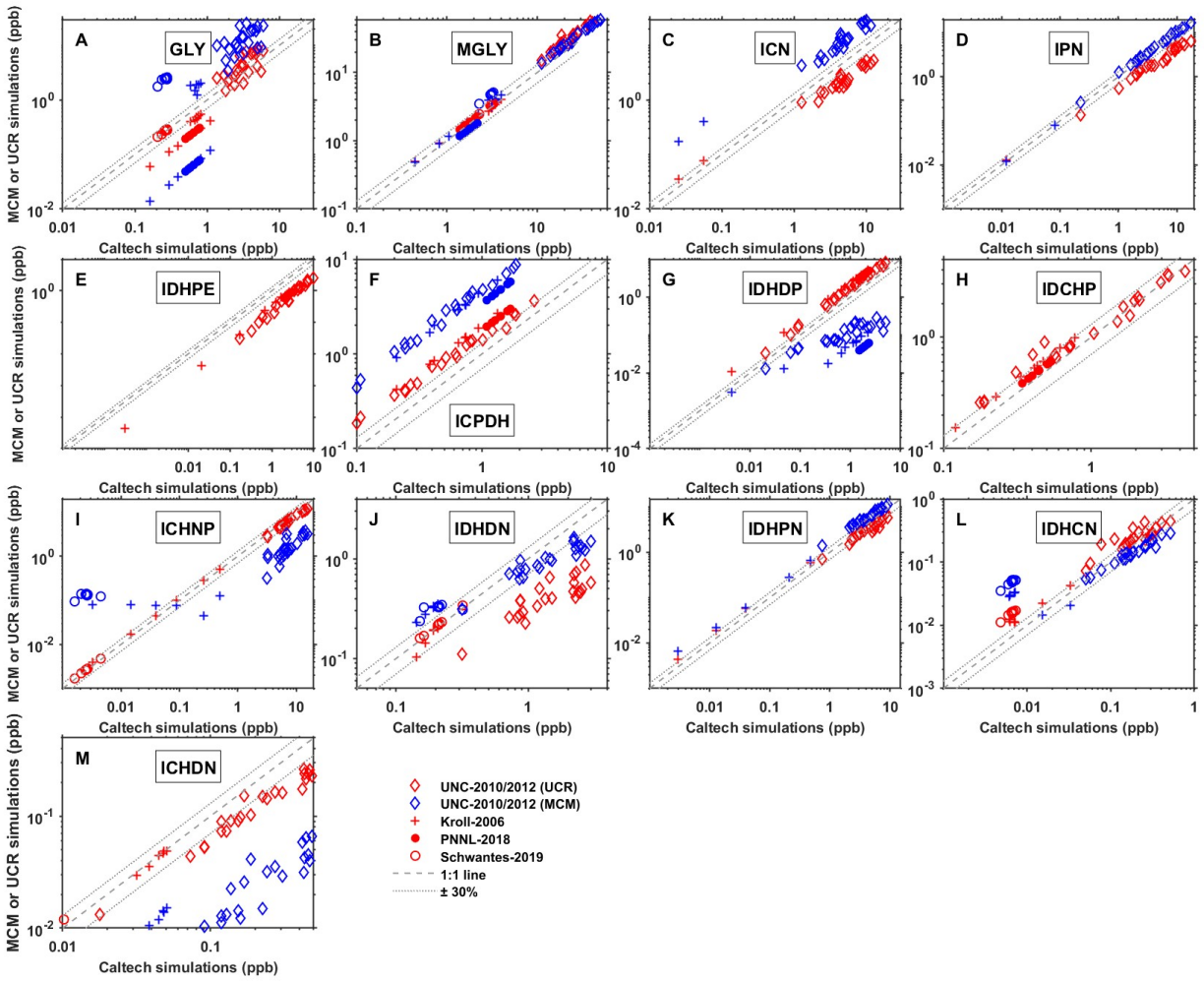

131

132 **Figure S1.** Comparison of simulated and measured species' maximum concentrations from
133 different chemical mechanisms. The *x*-axis represents maximum concentrations from Caltech
134 mechanism and y-axis represents values from UCR-ISOP (red markers) or MCM mechanism (blue
135 markers). Different marker types represent different chamber studies.

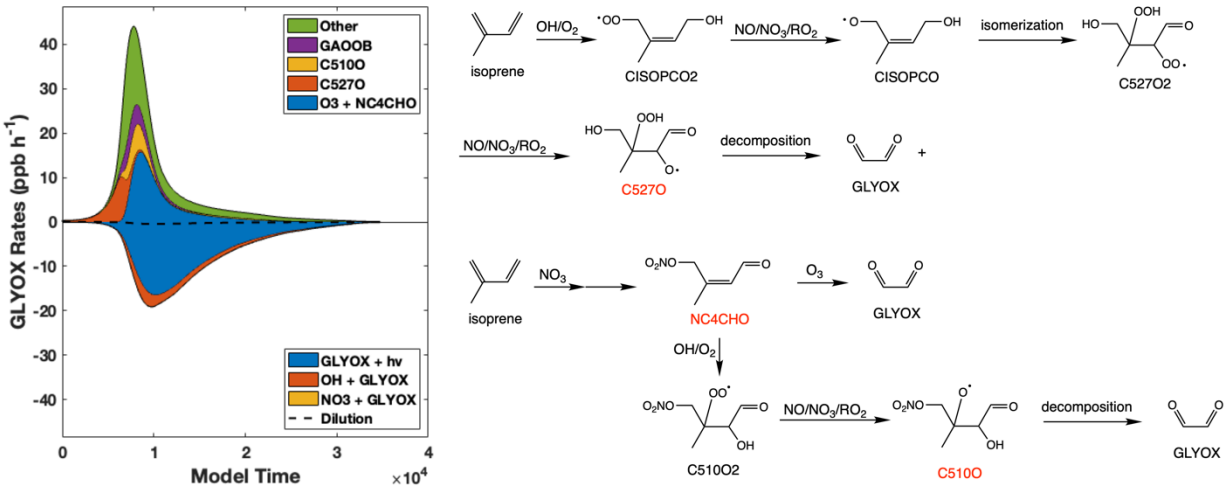

136

137 **Figure S2.** Left panel: major contributors to the formation and consumption of glyoxal (GLYOX)

138 in the MCM mechanism. Right panel: MCM pathways leading to glyoxal formation.

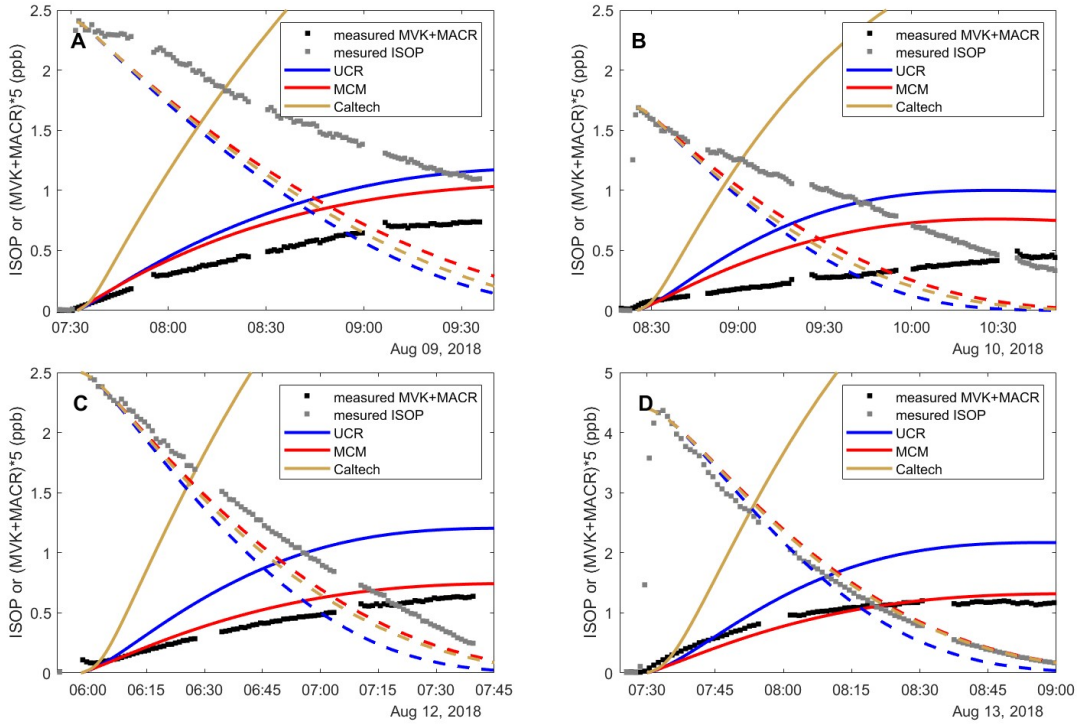

139

140 **Figure S3.** The simulation of Carlsson-2023 chamber study using different chemical mechanisms.
141 The Caltech mechanism largely overpredict the concentration of MVK+MACR compared to
142 measurements. The isoprene decays were overpredicted in (a)-(c) possibly due to the uncertainties
143 in initial isoprene and NO_3 concentrations.

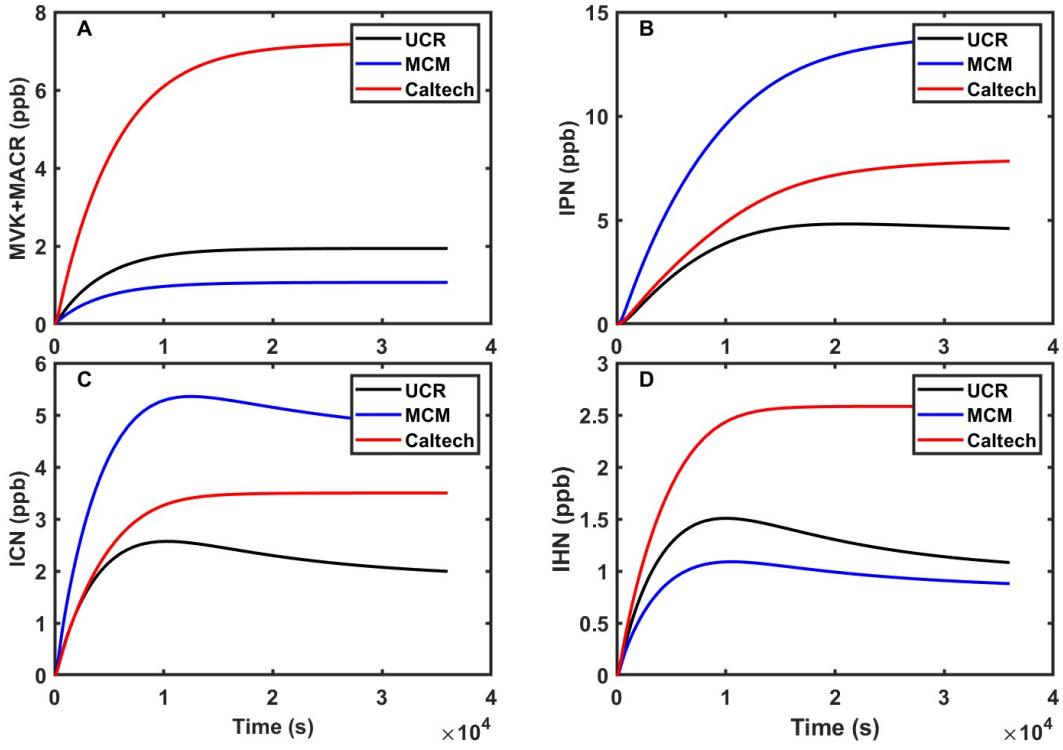

Figure S4. The simulation of Experiment 8 in Schwantes-2015 chamber study using different chemical mechanisms. (a) is the comparison of MVK+MACR; (b) is the comparison of hydroperoxide nitrates (IPN); (c) is the carbonyl nitrates (ICN) and (d) is the hydroxyl nitrates (IHN). In comparison to the measurements (see Schwantes et al. (2015) Fig. 2), the simulated IPN is slightly higher (5 ppb vs. 4 ppb); the simulated ICN is higher by a factor of ~2 (2 ppb vs. 1.2 ppb); and IHN is similar (~ 1 ppb). The later decreases in the UCR-ISOP and MCM mechanisms are due to further oxidation, which is not included in the Caltech mechanism.

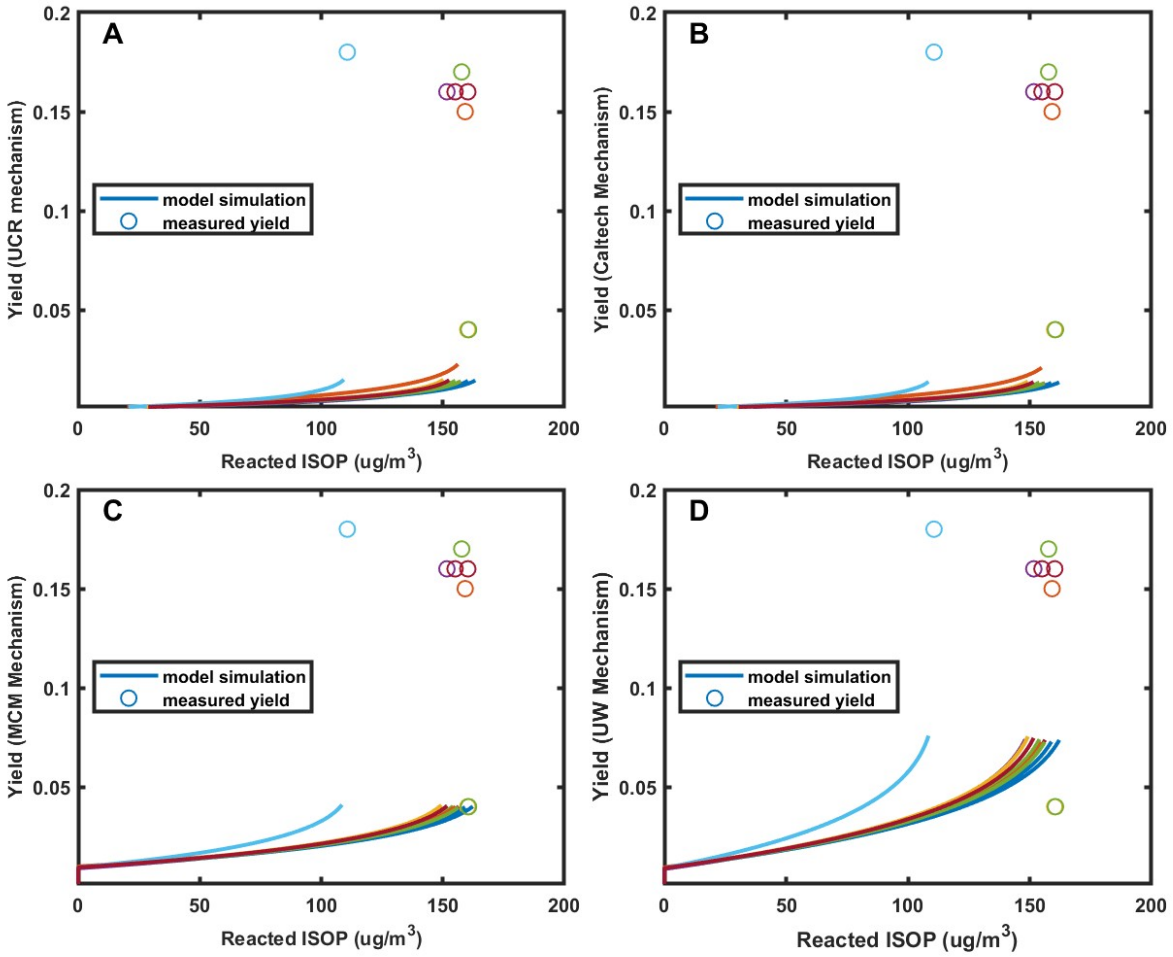

152

153 **Figure S5.** Model predicted isoprene SOA yield using different chemical mechanisms for
154 Schwantes-2019 chamber study under high-NO_x conditions. Different colors represent different
155 experimental runs. Experimental conditions for each run can be found in Table S5. The yield is
156 calculated from the modeled gas phase concentrations of IDHDN, IDHPN, IDHPN, ICHNP,
157 IDHCN and ICHDN assuming they can entirely partition into particle phase.

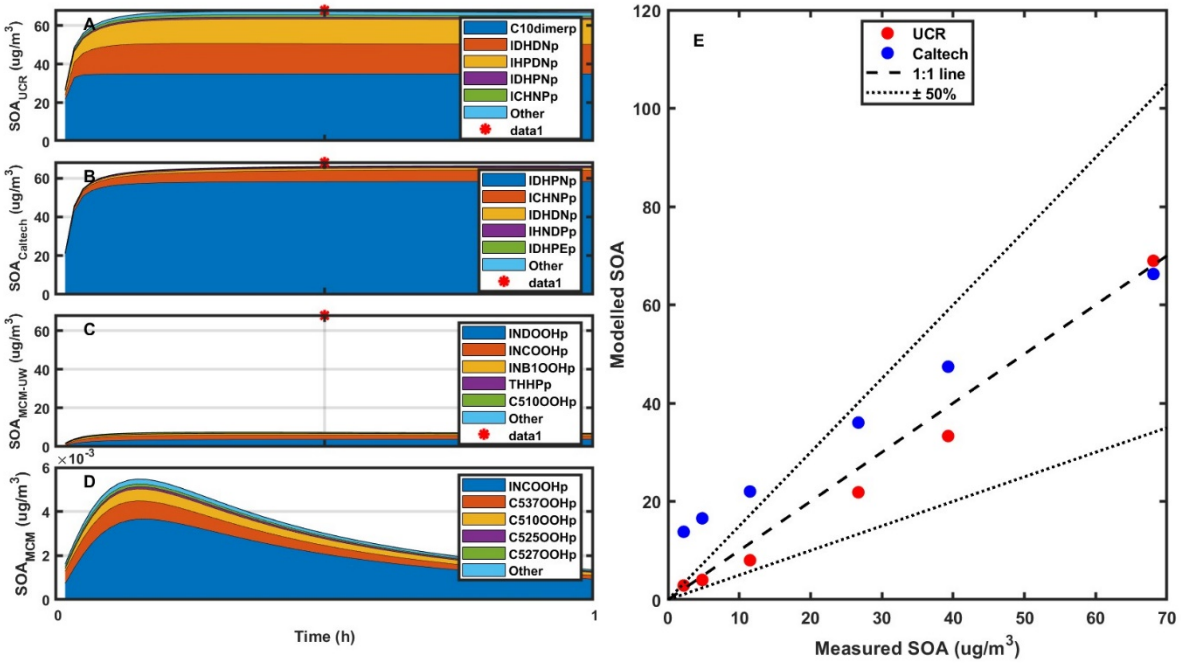

158

159 **Figure S6.** (a-d) The chemical constituents of modeled isoprene SOA in the Ng-2008 chamber
160 study using different chemical mechanisms: (a) UCR-ISOP; (b) Caltech; (c) MCM-UW; and (d)
161 MCM. In the MCM-UW mechanism, INDOOH, INCOOH and INB1OOH correspond to three
162 isomers of IDHPN in UCR-ISOP mechanism; THHP correspond to the species with three -OH
163 functional groups and one -OOH functional group. The species corresponding to the names in (c-
164 d) can be found in MCM website (https://mcm.york.ac.uk/MCM). (e) The comparison of modeled
165 SOA and measured SOA using UCR-ISOP and the Caltech mechanism.

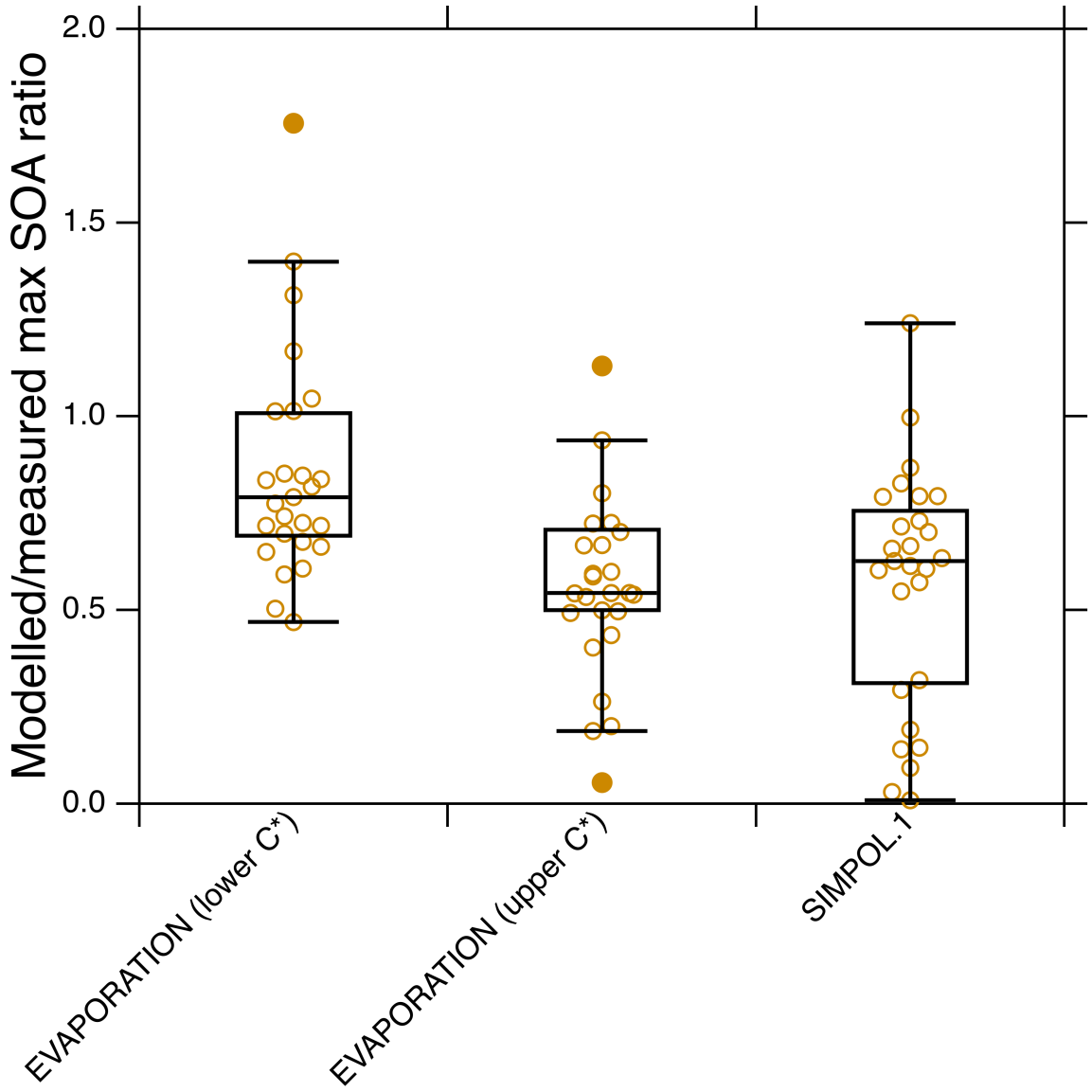

166

167 **Figure S7**. The distribution of modelled/measured SOA ratio using different vapor pressure
168 estimation methods. The data used includes Kroll-2006, PNNL-2018, PNNL-2014 and Ng-2008
169 chamber experiments. For each box, the central horizontal line in the box indicates the median,
170 and the bottom and top edges of the box indicate the 25th and 75th percentiles, respectively. The
171 whiskers extend to the most extreme data points not considered outliers, and the outliers are plotted
172 using the solid circle markers (other data points plotted using open circle markers).

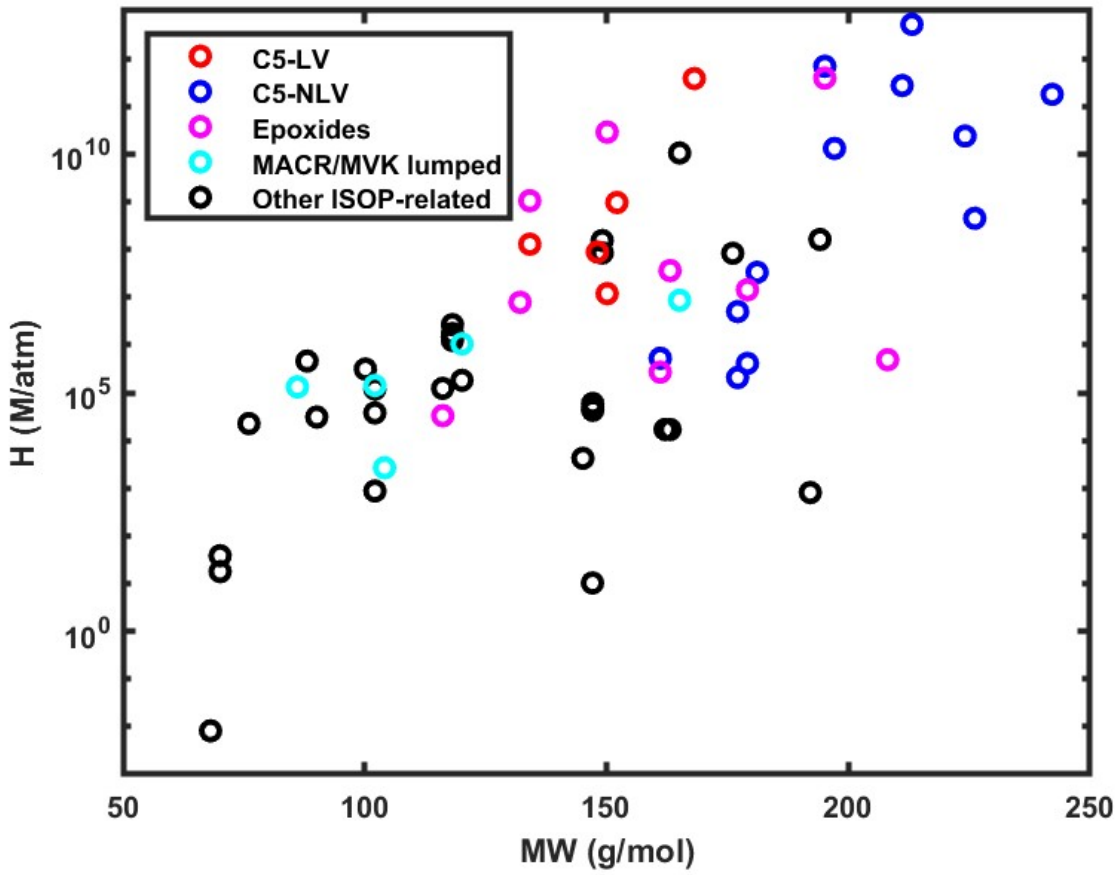

173

174 **Figure S8**. The distribution of Henry's law constants (H_{aq}) and molecular weight (MW) for
175 isoprene oxidation products. Different colors represent different groups, e.g., the red open circles
176 represent those five-carbon low-volatile species without nitrogen (C5-LV) and the blue open
177 circles represent those five-carbon nitrogen-containing low-volatile species (C5-NLV).

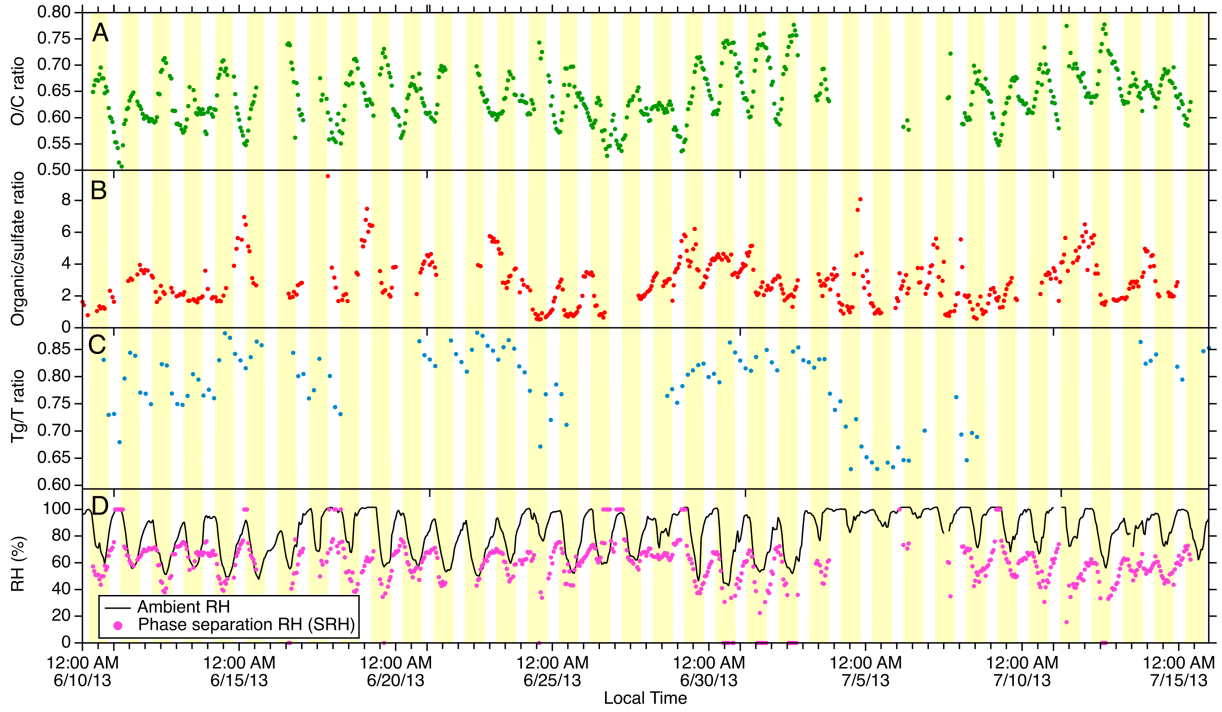

178

179 **Figure S9**. The time series of (A) measured O/C ratio, (B) organic aerosol/sulfate ratio, (C) glass

180 transition temperature (T_g) over ambient temperature (T) (Schmedding et al., 2020), and (D)

181 predicted phase separation RH (SRH) and ambient RH.

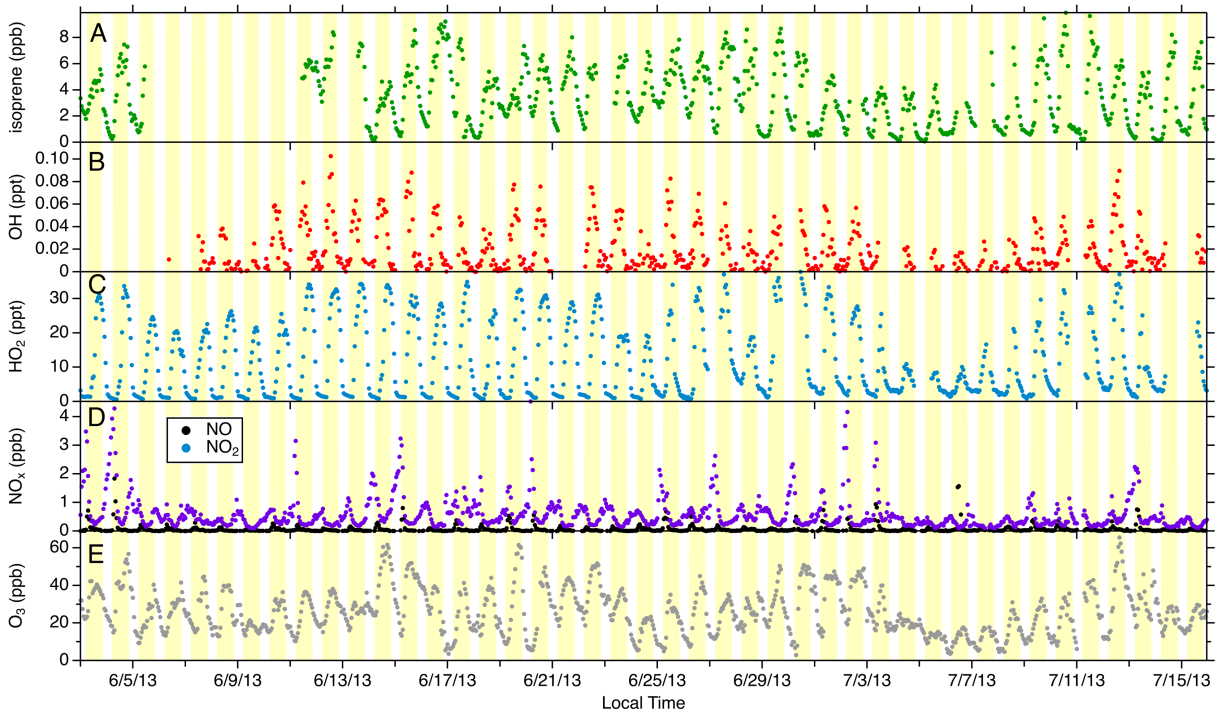

Figure S10. The time series of (A) isoprene, (B) OH, (C) HO_2, (D) NO and NO_2, and (E) O_3 during the SOAS field campaign.

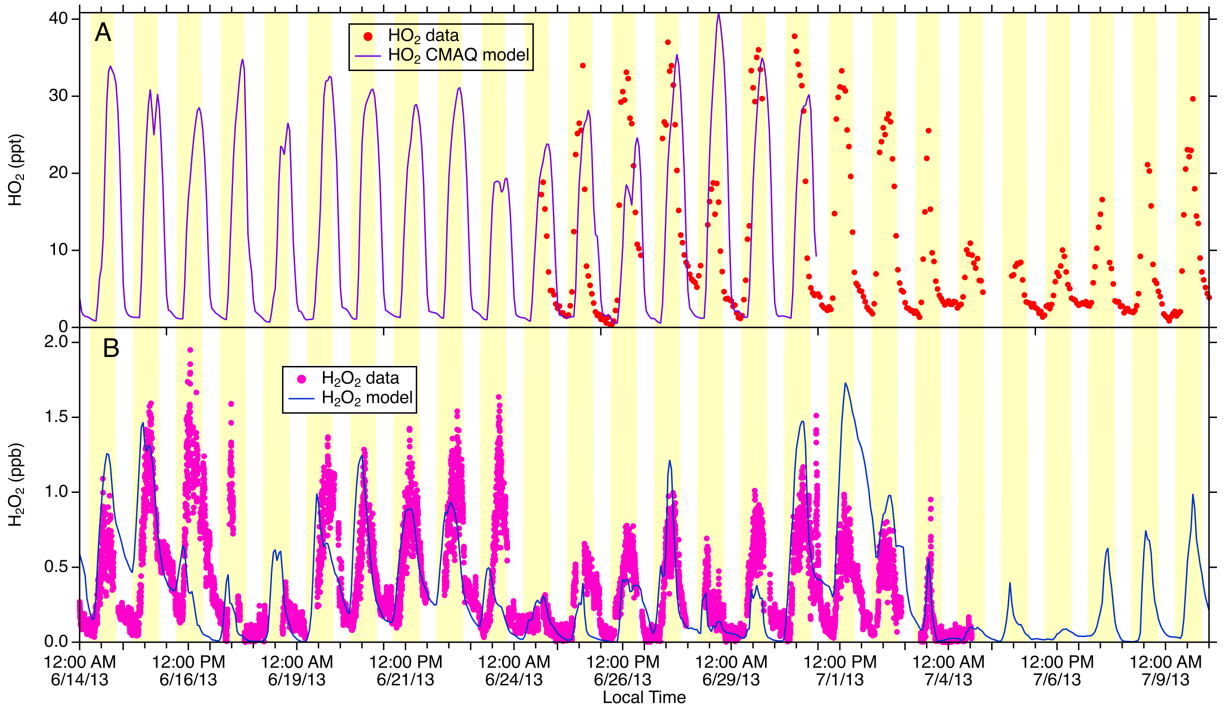

185

186 **Figure S11**. The time series of (A) measured and CMAQ modelled HO_2, (B) measured and

187 modeled H_2O_2 concentrations for the SOAS field campaign.

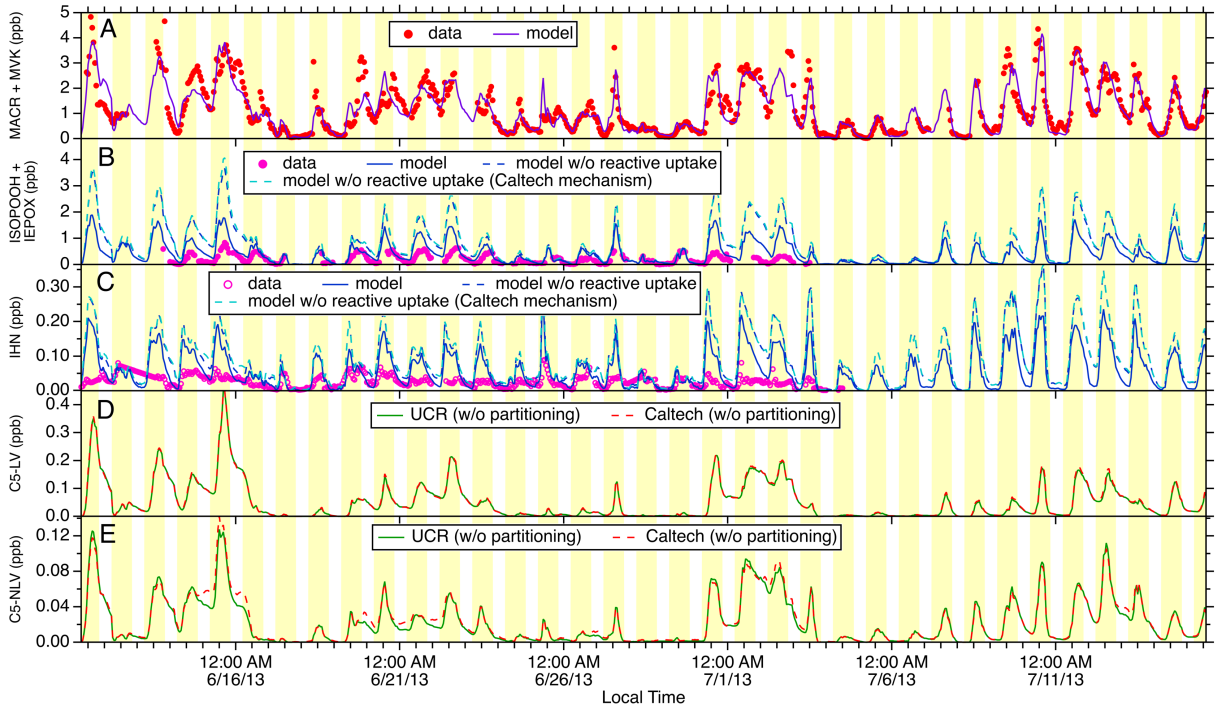

188

189 **Figure S12**. The time series of (A) measured and modeled MVK+MACR using UCR-ISOP; (B)
190 measured and modeled IEPOX+ISOPOOH using both the UCR-ISOP and Caltech mechanisms,
191 wherein for the UCR-ISOP simulations, the scenario considering IEPOX reactive uptake is also
192 shown; (C) measured and modeled IHN using both the UCR-ISOP and Caltech mechanisms,
193 wherein for the UCR-ISOP simulations, the scenario considering 1,2-IHN reactive uptake is also
194 shown; (D) modeled C5-LV; and (E) modeled C5-NLV. The comparative gas-phase simulations
195 between the UCR-ISOP and Caltech mechanisms suggest that the measurement-model
196 disagreement is not due to any specific mechanism, but rather a lack of understanding of processes.

197

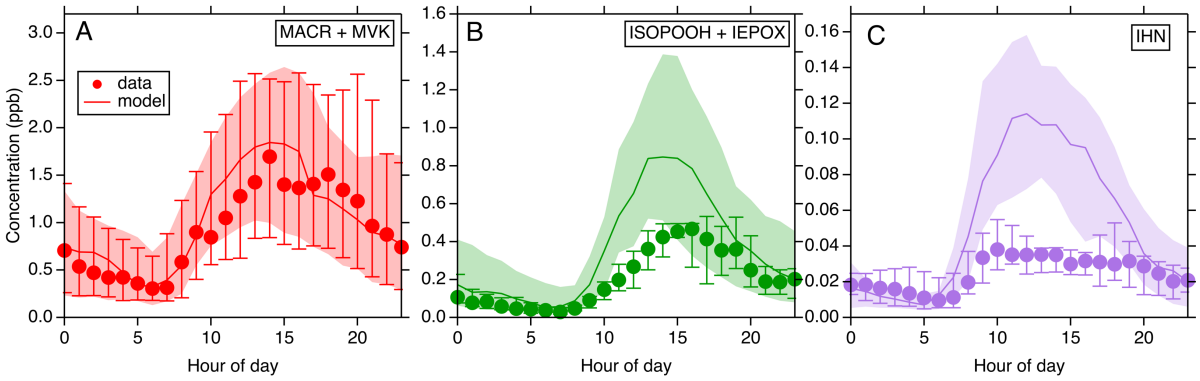

198

199 **Figure S13**. Measurement-simulation comparisons of the diurnal variations for (A) MACR +

200 MVK; (B) ISOPOOH + IEPOX; and (C) IHN. The error bars represent the 25th and 75th percentiles

201 of the measurements and the shaded areas represent the 25th and 75th percentiles of the simulations.

202 The simulations exhibit very good agreement for measured MACR + MVK (A), but over predict

203 ISOPOOH + IEPOX by a factor of ~ 1.8 and IHN by a factor of 1.9 (average of median values).

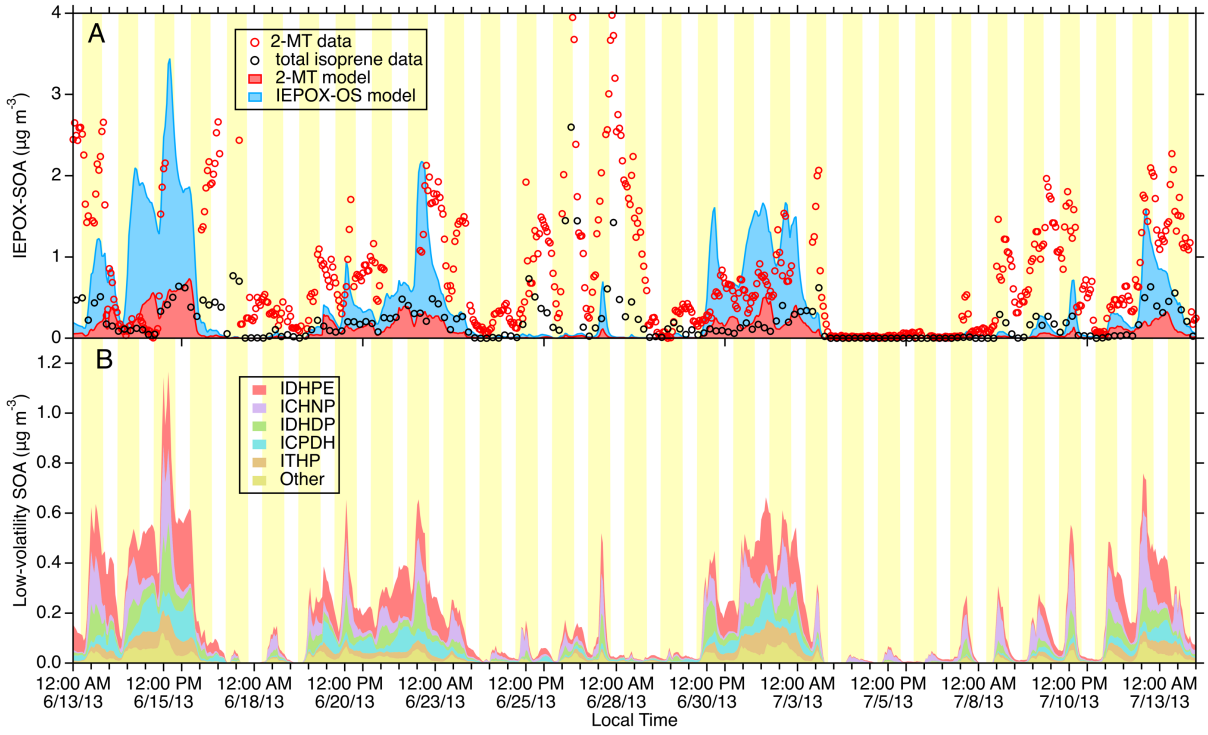

204

205 **Figure S14**. The time series of (A) measured (by FIGAERO-CIMS and GC×GC-MS) and

206 modelled IEPOX-derived SOA using the UCR-ISOP mechanism and (B) modelled isoprene SOA

207 from the low-volatility pathways.

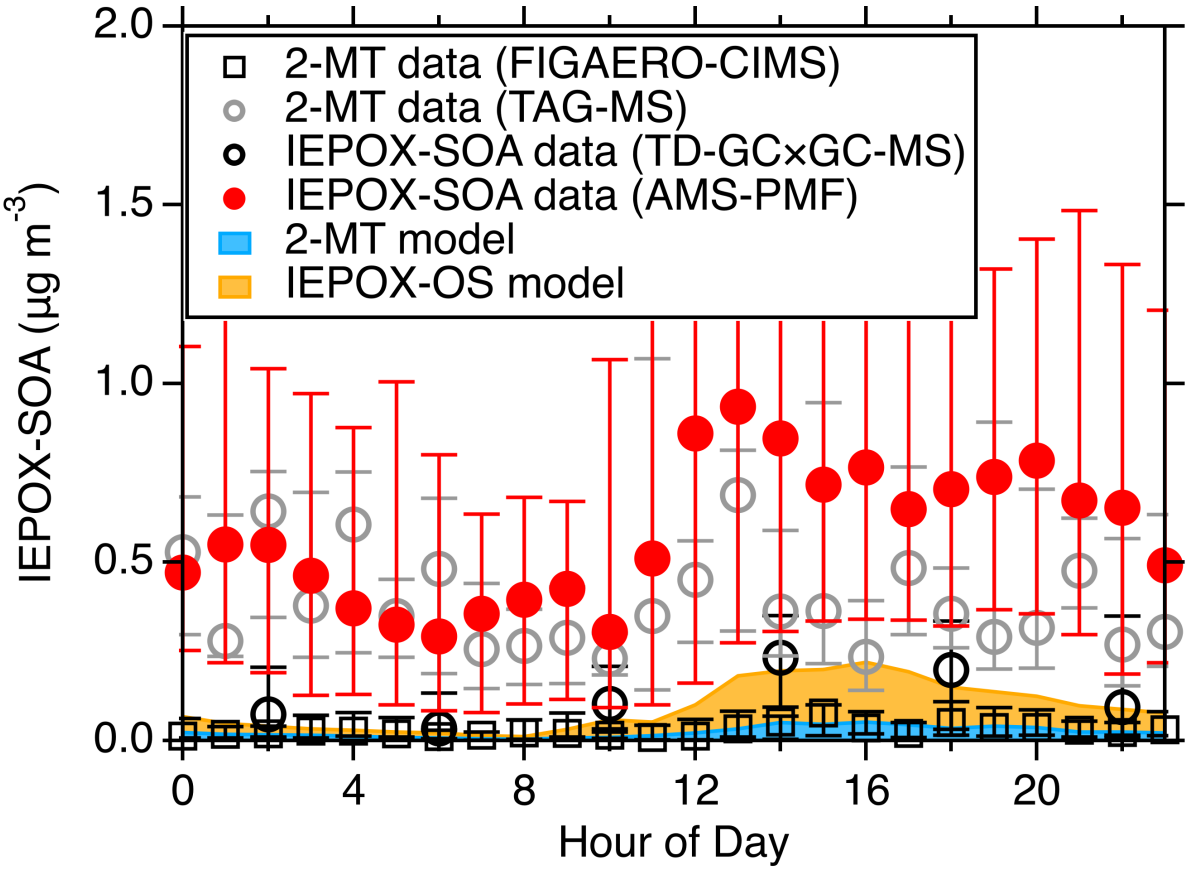

208

209 **Figure S15**. The diurnal trend of IEPOX-SOA comparison between the measurements and

210 simulations, reproduced from Fig. 5A, but including the TAG-MS measurements and the IEPOX-

211 SOA factor from AMS-PMF analysis.

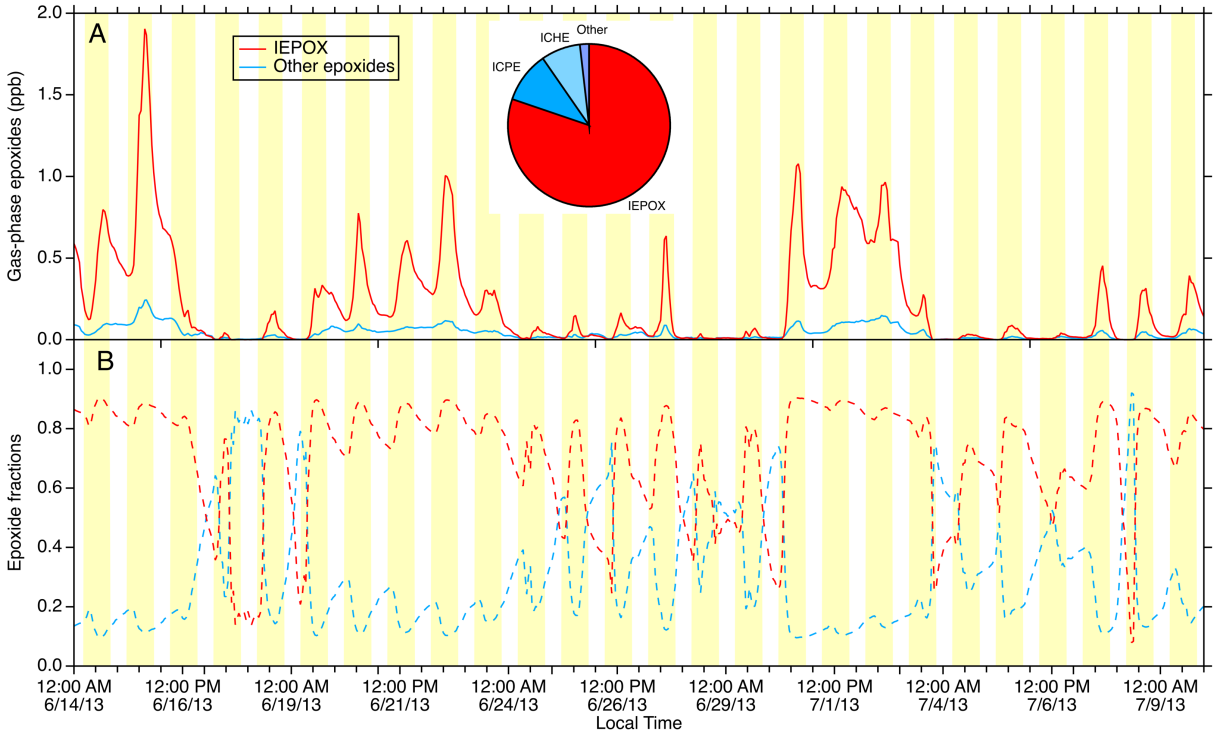

212

213 **Figure S16**. The time series of model predicted IEPOX and summed other epoxides for (A)
214 concentrations and (B) relative fractions. Note, IEPOX is the sum of both β- and δ-IEPOX; the
215 summed other epoxides do not include IDHPE, which is considered a C5-LV species. The insert
216 pie chart shows the contributions of major epoxides for SOAS medians, where IEPOX account for
217 80%.

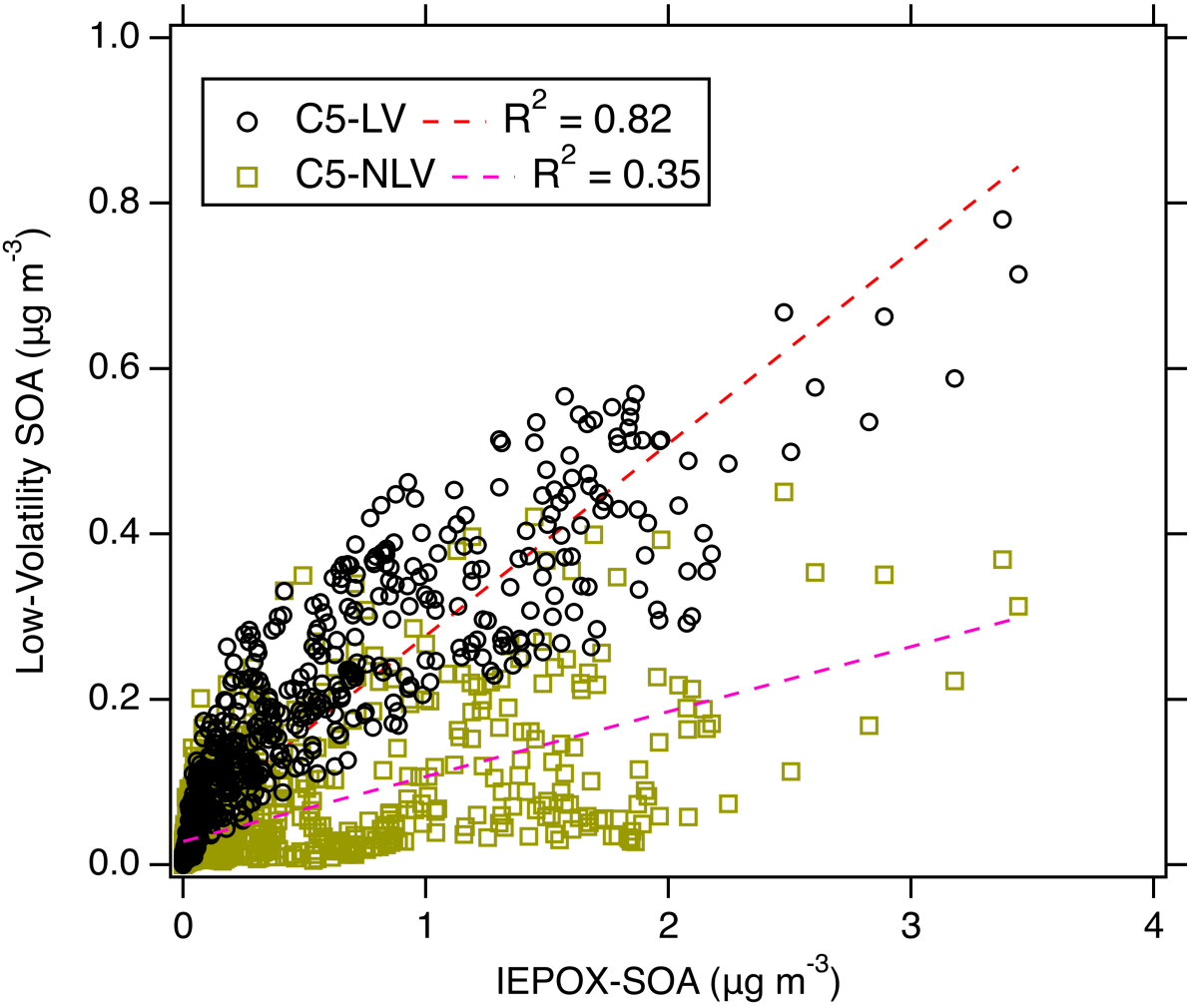

Figure S17. The correlation between the simulated SOA from IEPOX reactive uptake and those from low-volatility species (C5-LV and C5-NLV). The R2 values are 0.82 for C5-LV and 0.35 for C5-NLV.

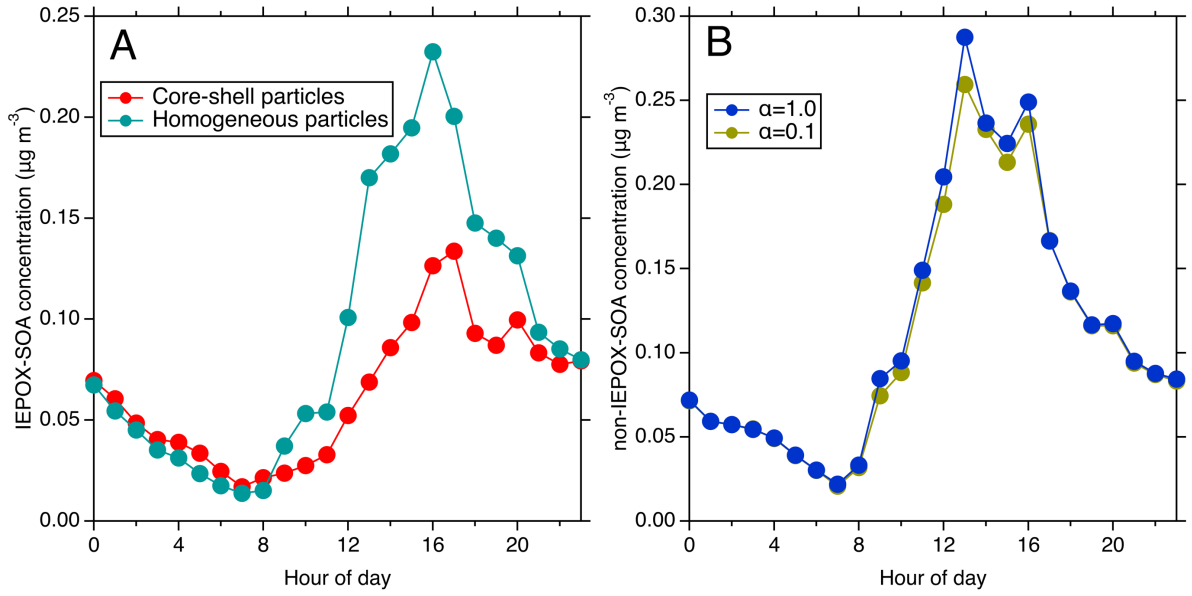

222

223 **Figure S18**. The sensitivity tests of (A) modelled IEPOX-SOA under assumptions of
224 homogeneous particles vs. core-shell particles, and (B) modelled non-IEPOX-SOA under
225 assumptions of $\alpha = 1$ (without diffusion limitation) vs. $\alpha = 0.1$ (with diffusion limitation). In (A),
226 the organic and inorganic mass concentrations from AMS data are used to derive particle's core
227 and shell thickness, with the assumption that the organic shell contains 10% of the aerosol-
228 associated liquid water content and the inorganic core 90%. The products of H_{org} (Henry's law
229 coefficient in the organic layer) and D_{org} (diffusion coefficient of IEPOX in the organic layer) are
230 extrapolated from experimental results in Zhang et al. (2018).

231

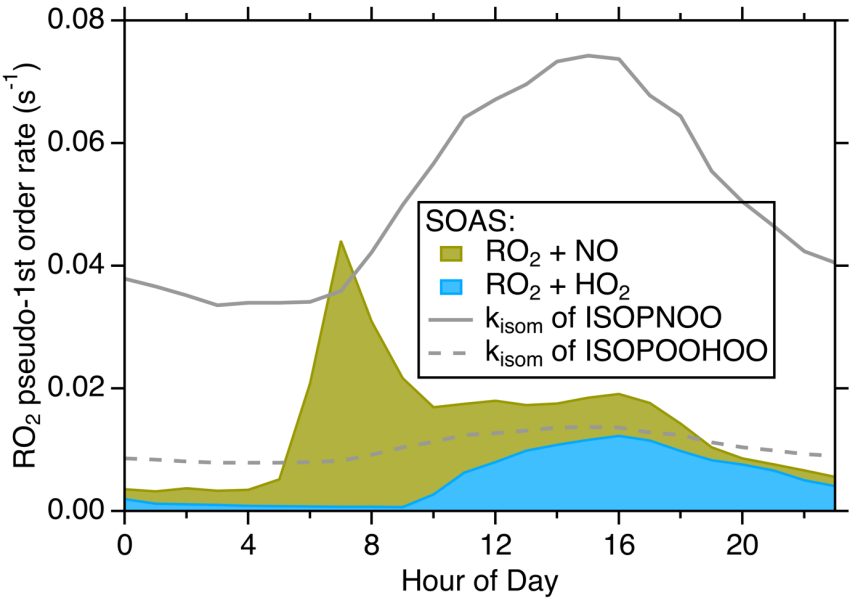

232

233 **Figure S19**. Pseudo-first order rates for RO_2 bimolecular reactions with NO and HO_2 during

234 SOAS, in comparison with the unimolecular isomerization rate constants for ISOPNOO and

235 ISOPOOHOO.

References

Kamens, R. M., Zhang, H., Chen, E. H., Zhou, Y., Parikh, H. M., Wilson, R. L., Galloway, K. E., and Rosen, E. P.: Secondary organic aerosol formation from toluene in an atmospheric hydrocarbon mixture: Water and particle seed effects, Atmospheric Environment, 45, 2324-2334, 2011.

Schmedding, R., Rasool, Q. Z., Zhang, Y., Pye, H. O. T., Zhang, H., Chen, Y., Surratt, J. D., Lopez-Hilfiker, F. D., Thornton, J. A., Goldstein, A. H., and Vizuete, W.: Predicting secondary organic aerosol phase state and viscosity and its effect on multiphase chemistry in a regional-scale air quality model, Atmos. Chem. Phys., 20, 8201-8225, 10.5194/acp-20-8201-2020, 2020.

Schwantes, R. H., Teng, A. P., Nguyen, T. B., Coggon, M. M., Crounse, J. D., St. Clair, J. M., Zhang, X., Schilling, K. A., Seinfeld, J. H., and Wennberg, P. O.: Isoprene NO3 Oxidation Products from the RO2 + HO2 Pathway, The Journal of Physical Chemistry A, 119, 10158-10171, 10.1021/acs.jpca.5b06355, 2015.

Thornton, J. A., Shilling, J. E., Shrivastava, M., D'Ambro, E. L., Zawadowicz, M. A., and Liu, J.: A Near-Explicit Mechanistic Evaluation of Isoprene Photochemical Secondary Organic Aerosol Formation and Evolution: Simulations of Multiple Chamber Experiments with and without Added NOx, ACS Earth and Space Chemistry, 4, 1161-1181, 10.1021/acsearthspacechem.0c00118, 2020.

Zhang, H., Parikh, H. M., Bapat, J., Lin, Y.-H., Surratt, J. D., and Kamens, R. M.: Modelling of secondary organic aerosol formation from isoprene photooxidation chamber studies using different approaches, Environmental Chemistry, 10, 194-209, https://doi.org/10.1071/EN13029, 2013.

Zhang, H., Rattanavaraha, W., Zhou, Y., Bapat, J., Rosen, E. P., Sexton, K. G., and Kamens, R. M.: A new gas-phase condensed mechanism of isoprene-NOx photooxidation, Atmospheric Environment, 45, 4507-4521, https://doi.org/10.1016/j.atmosenv.2011.04.011, 2011.

Zhang, X., Cappa, C. D., Jathar, S. H., McVay, R. C., Ensberg, J. J., Kleeman, M. J., and Seinfeld, J. H.: Influence of vapor wall loss in laboratory chambers on yields of secondary organic aerosol, Proceedings of the National Academy of Sciences, 111, 5802-5807, doi:10.1073/pnas.1404727111, 2014.

Zhang, Y., Chen, Y., Lambe, A. T., Olson, N. E., Lei, Z., Craig, R. L., Zhang, Z., Gold, A., Onasch, T. B., Jayne, J. T., Worsnop, D. R., Gaston, C. J., Thornton, J. A., Vizuete, W., Ault, A. P., and Surratt, J. D.: Effect of the Aerosol-Phase State on Secondary Organic Aerosol Formation from the Reactive Uptake of Isoprene-Derived Epoxydiols (IEPOX), Environmental Science & Technology Letters, 5, 167-174, 10.1021/acs.estlett.8b00044, 2018.